P3.6

DETECTION OF A GLOBAL AND CARIBBEAN CLIMATE CHANGE

[1]Nazario D. Ramirez-Beltran*, [1]Oswaldo Julca, and [2]Jorge Gonzalez
[1]University of Puerto Rico, Mayaguez, PR 00680
[2]Santa Clara University, Santa Clara, CA 95053

1. INTRODUCTION.

The Earth has been experimented several climate changes, which have been documented by several researchers (Huntingford et al 2006, Hansen 2005, Easterling et al 2000, Battisti el al 1997, She and Krueger 2004, and Barnett et al 1999). The global warming is affecting human lives and economy, and particularly on agriculture and forestry (Salinger 2005). Easterling et al (2000) pointed out that in the United States and since 1987 more than 360 weather events have produced losses in excess of $5 million each event with several catastrophic consequences. The temperature in globe has increased during the last 140 years, due to the fact that the number of heat waves has increased (Schar et al 2004, Changnon et al 2000). The global warming is a real event and is causing catastrophic consequences.

The following researches established that the global warming is due to anthropogenic sources (Huntingford et al 2006, Hansen 2005, Easterling et al 2000). The International Project of Climate Change (IPCC) states that the balance of evidence suggests a discernible human influence on global climate (IPCC, 2001). The anthropogenic activities that affect the global warming are the emission of greenhouse gases and changes in land use, such as urbanization and agriculture. Other researchers state that the global warming may be attributed to natural variability, which can be observed in the energy transported by the atmosphere, ocean and their respective circulation (Battisti el al 1997). Other natural variability is the volcanic eruption, and the solar flux variability (She and Krueger 2004, Barnett et al 1999).

People have been simulated some possible scenarios to represent the most probable future consequences (IPCC 2001, Angeles 2005, Huntingford et al 2006, Hansen 2005). It has been shown that predicting Earth surface temperature is almost impossible since the anthropogenic and the natural variability include a large amount of uncertainties that are difficult to predict (Stott & Kettleborough 2002).

There are several techniques that have been used to detect climate changes. The available climate change detection algorithms use different statistical techniques such as: optimal finger print, pattern recognition, trend identification, time-varying patterns, correlation and regression techniques (Easterling et al. 1997, Barnett et al. 1999, Feldstein 2002, Schar 2004, IPCC 2001, Smith et al 2002,.). A new algorithm was proposed to detect a climate change (Ramirez and Julca, 2006). This algorithm uses a time series as a climate indicator to determine whether or not there is a significant change on the underlying climate indicator. The algorithm identified three major components of the climate indicator: the trend, the seasonal, and the stochastic component. The algorithm removes trend and seasonal components and identifies whether or not the stochastic component exhibits a significant autocorrelation structure. Finally the autocorrelation structure is removed to obtain the stochastic independent time series, which is processed by a sequential statistical test to identify the presence of a significant climate change. The proposed algorithm is based on the assumption that the times series of the climate indicator has no errors.

People have either attributed the global changes to a natural variability or to anthropogenic causes. We want to explore whether or not our proposed algorithm is able to detect Global and Caribbean climate changes. We would also like to determine whether or not the identified climate changes occurred at the same time when either a natural change or a human induced change has occurred.

The second section of this paper describes the studied climate indicators. The third section presents the proposed methodology. The fourth section presents some preliminary results and the last section presents some conclusions.

2. CLIMATE INDICATOR DATA

Five data sets were studied in this research. Two data sets are associated to possible causes of climate change, which are called attribution variables and three climate

Corresponding authors address: Nazario D. Ramirez, University of Puerto Rico, Dpto. Industrial Engineering, Mayaguez, PR, 00680, e-mail: nazario@ece.uprm.edu

indicators. The attribution variables are the solar radiation and CO_2 emissions. The data climate indicators are surface temperature, sea level and cloud cover.

2.1 Attribution variables

a) Sunspots. The Earth is receiving the radiation from the sun and consequently changes on the Earth surface temperature may be attributed to sun activity. Satellite data has been used to prove that solar radiation can be measured by studying the behavior of sunspots. Figure 1 shows the observed sunspot during the period 1979-2005 and the observed solar irradiance. This figure shows that the solar activity can be study by analyzing the behavior of sunspots.

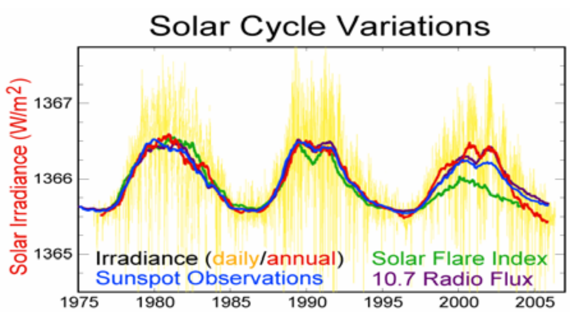

Figure 1 The behavior of the solar irradiance, sunspots, solar flare activity, and 10.7 cm radio flux.

The time series of sunspots was obtained from the Royal Observatory of Belgium (http://sidc. oma.be/sunspot-data/), The selected period includes from Jan 1880 until Aug 2006 (see Figure 2). This period was selected because the available surface time series contains exactly the same period of time.

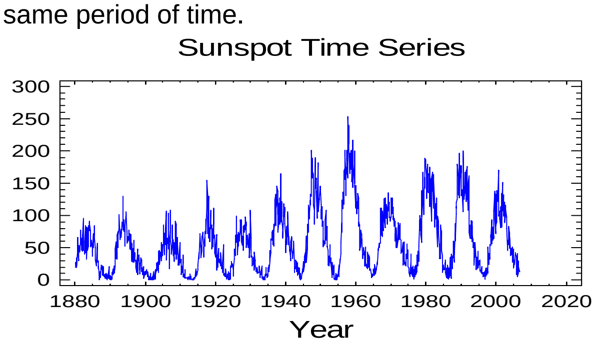

Figure 2 The sunspot has a period of approximately 127 months which is equal 11.5 years. This time series shows 12 periods along the total time series.

b) Carbon Dioxide. The carbon dioxide time series was obtained from Mauna Loa station Hawaii. This data set includes the period from January 1958 to August 2006. Figure 3 shows the behavior of the CO_2. This data constitute the longest continuous record of CO_2 concentrations available in the world. This climate indicator is considered as one of the most favorable locations for measuring undisturbed air because the local influences of vegetation and human activities are minimal over CO_2 concentrations. It should be noted that the volcanic events are excluded from the records (Keeling and Whorf 2005). The CO_2 time series was obtained from the following web site: http://cdiac.ornl.gov/ftp/trends/co2/maunaloa.co2.

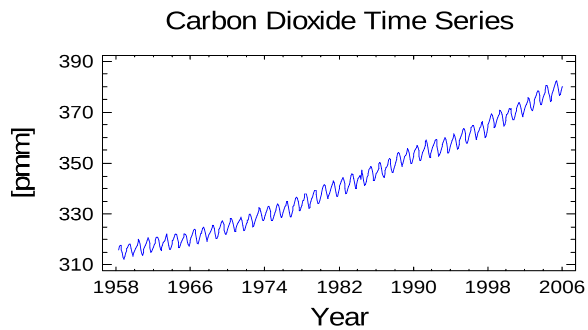

Figure 3 The carbon dioxide time series (ppm) from January 1958 to August 2006 obtained from Mauna Loa Station, Hawaii.

2.2 Climate indicators

a) Global Surface Temperature. The global surface temperatures were provided by the Goddard Institute for Space Studies (GISS). The anomalies of global surface temperature data were acquired at the web site http://data.giss. nasa.Gov/gistemp/. Figure 4a shows the anomalies of the global land surface temperature. Figure 4b shows the anomalies of land and ocean surface temperature. Figure 4c shows the land surface land temperature over the North Hemisphere. These data sets include the following period from Jan 1880 to Aug 2006.

The surface data set was developed based on the Global Historical Climatology Network (GHCN), and the development and analysis of this data set is described by Hansen and Ruedy (1999),

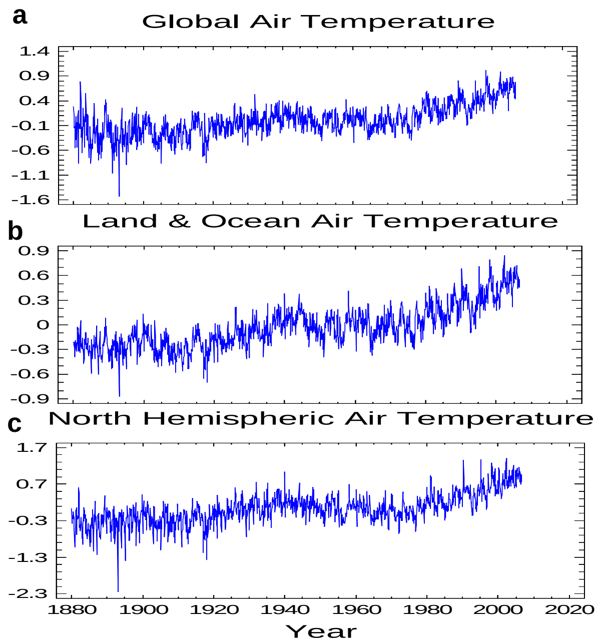

Figure 4 Anomalies of the surface temperature. a, global land surface temperature. b, global land and ocean surface temperature, and c, north hemispheric land surface temperature.

Caribbean Air Temperature. Air temperatures for the major Caribbean islands were obtained from GHCN 2. The study Caribbean islands are: Cuba (CU), Jamaica (JA), Puerto Rico (PR), and La Espanola, which includes Dominican Republic (DR) and Haiti (HA). PR is the Caribbean island with a large amount of meteorological stations. PR has 14 stations that belong to GHCN and 39 that are administered by the National Weather Services (COOP stations) and makes a total of 53 stations. Table 1 shows the summary of available stations that were used in this work. The monthly air temperature includes the following period: from 1948 to present (2006).

Table 1 Number of stations over the Caribbean area.

Country	Cuba	Dominican Republic	Haiti	Jamaica	Puerto Rico
Number of stations	14	28	1	5	53

Figure 5 shows the monthly air temperature for PR. This figure shows the average, maximum and minimum monthly air temperature. Figure 6 shows the average air temperatures based on 14 stations and maximum and minimum air temperature for Guantanamo station. Figure 7 shows the air temperature from Dominican Republic, Haiti, and Jamaica.

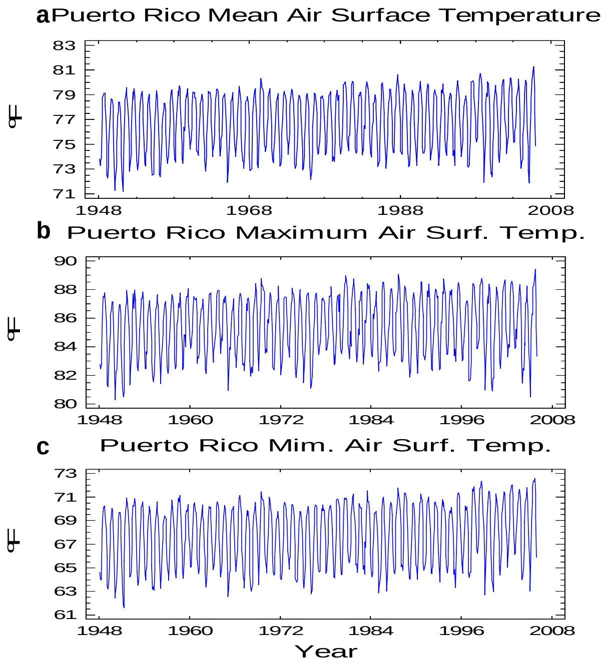

Figure 5 The average air temperature (AT) of Puerto Rico from Jan 1948 until Dec 2005. a, the mean AT was obtained from 53 stations data. b, to maximum AT was calculated from 42 stations, and. c, the minimum AT was computed with 42 stations. This data were extracted from COOP and GHCN 2 stations.

The surface air temperature from the NCEP/NCAR reanalysis data were used as a proxy variable to estimate some of the missing values that we encounter in some stations. The nearest grid points to each island were used to derive a regression equation between the observed air temperature by the stations and the NCEP temperature estimated at 0, 6, 12, 18 universal times. The regression equations exhibit an average of 0.9 of correlation coefficient. The NCEP values at 6 and 18 hours were used as a proxy variable to estimate the minimum and maximum air temperature at stations, respectively.

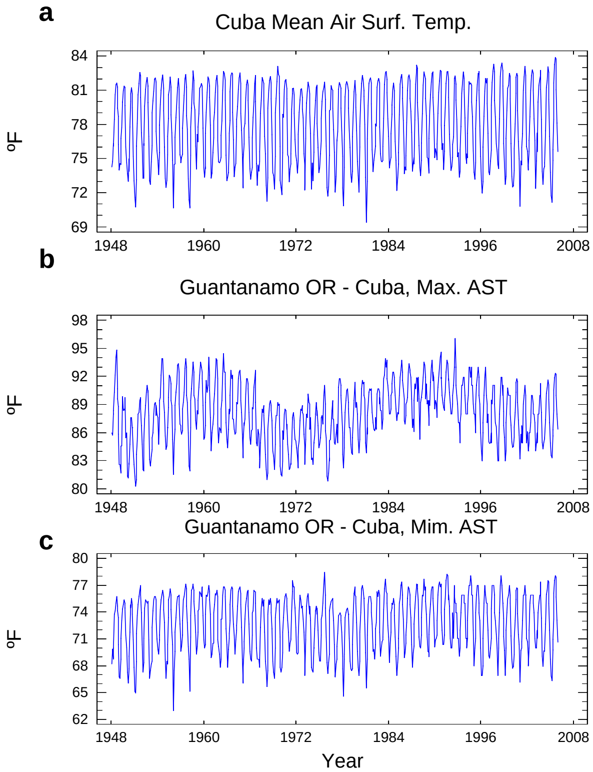

Figure 6 The average AT for Cuba from Jan 1948 until Dec 2005. **a**, the mean AT was computed from 14 stations. **b**, the maximum AT for Guantanamo station, and **c**, the minimum AT for Guantanamo station, 1. This data was extracted from GHCN 2.

b) Global and Caribbean Cloud Cover. The cloud cover monthly time series was obtained from the International Satellite Cloud Climatology Project (ISCCP). The D2 product provides the properties of the clouds observed at every three hours and presented in monthly time series during the period of July 1983 to June 2005. Some of the included variables in this data set are: cloud cover, top-cloud temperature, top-cloud pressure, optical thickness, and water path. The clouds are classified based on optical thickness and on top pressure. The cloud products were generated from sensors located on 7 satellites. More information can be found in the following site: http://iridl.ldeo. columbia.edu /SOURCES /.NASA/. ISCCP/.D2/. Quispe (2006) developed a user friendly computer program to read and manage the cloud data files.

The global cloud cover file includes 6,596 grids and the cloud cover was obtained for each type of cloud according its elevation: low, middle, and high. The Caribbean area includes the following geographical location: latitude from 17N to 24N and longitude from 87W to 64W. Figure 8 shows the average Global and Caribbean cloud cover, from July 1983 until June 2005.

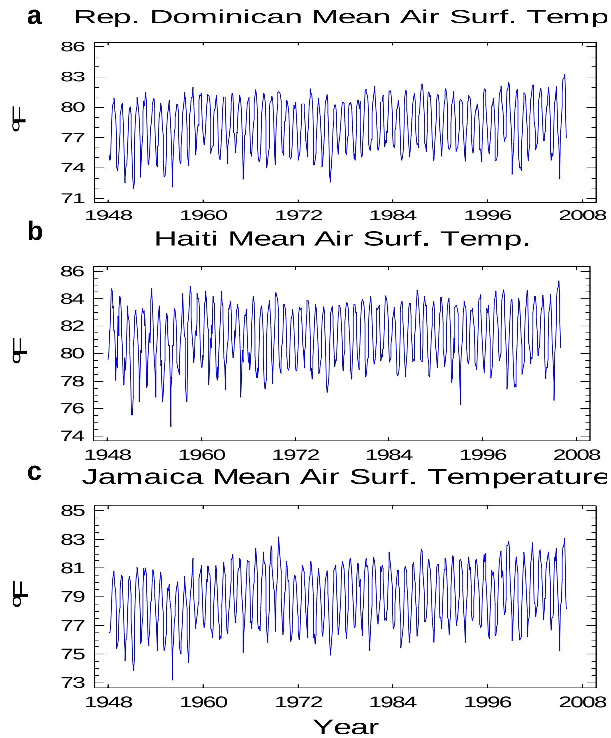

Figure 7 The average AT from Jan 1948 until Dec 2005. **a**, average AT for Dominican Republic was computed with 28 stations. **b**, the average AT for Haiti was based on a single station, and **c**, the average AT was computed with 5 stations. These data were extracted from GHCN 2.

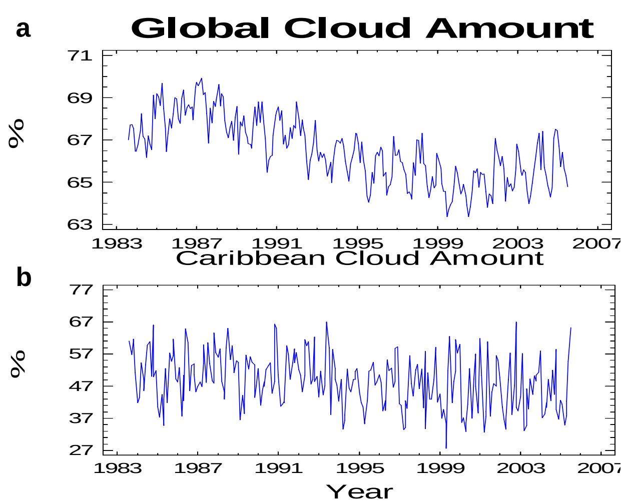

Figure 8 The average cloud amount from July 1983 until June 2005. **a**, Global, and **b**, Caribbean. This data was extracted from ISCCP D2.

c) Global and Caribbean Sea Level. The sea level data set were obtained from two satellites Topex and Jason. The global data includes monthly observations from 1992 to 2005 and the Caribbean data covers only from 1992 to 2002. The data can be obtained at the following web sit: http://sealevel.colorado.edu/results.Php. Additional information can be obtained at (Leuliette et al 2004). Figure 9 shows the global and Caribbean sea level measured in mm.

3. METODOLOGY

3.1. Climate change detection test

The proposed detection algorithm consists of removing trend, periodicity, and the autocorrelation structure of a climate indicator and determines whether or not the mean of the process changes over time. The algorithm consists of determining when the process changes from being a stationary to nonstationary process and includes five major steps: (1) collect the largest sequence of a climate indicator; (2) divide the data sets in two parts: the baseline and the testing sequence; (3) identify an autoregressive moving average model to the baseline; (4) computing the autoregressive moving average (ARMA) finger print; and (5) use a sequential hypothesis testing procedure to determine whether or not the mean of the process has changed. The sequential test also includes determining whether or not the autocorrelation structure changes over time.

a) Sequence of a climate indicator. It is assumed that climate properties of a given part of the world are expressed by a sequence of a climate indicator. A climate indicator can be expressed as a time series of air temperature, sea level, pressure, etc. It is required that the selected time series has no missing values and were obtained at equal time intervals. It is desirable that the time series will be large enough to identify the autocorrelation structure and left a significant part of the series in the testing side. The minimum length of the time sequence must be 50 observations.

b) Dividing the time series. The time series will be divided into two parts. The first part will be called the baseline and the second part will be called the testing part. The baseline will be used as a reference point to measure the change with respect to the baseline. The baseline must be at least 30 observations i.e. to be able to identify a time series model. The baseline will be located on the left and the testing part on the right hand side of the series. Typically, the baseline may be located at the beginning of the series; however, it could be placed in almost any part of the series as long as enough testing observations are available. The testing part will be at least 20 observations and will be used to measure whether or not there exists a significant change with respect to the baseline.

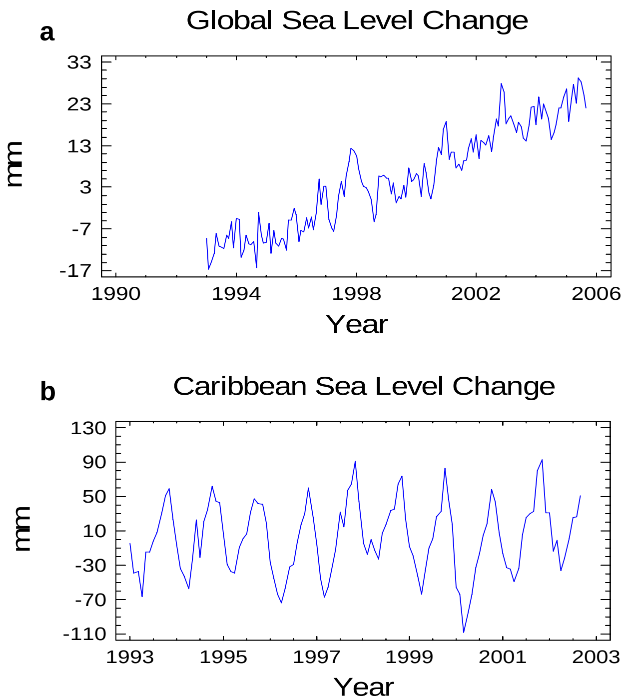

Figure 9 The average of sea level. **a**, Global from Dec 1992 until Aug 2005. **b**, Caribbean from Dec/1992 until Aug/2002. This data set was obtained from Topex/Jason.

It should be noted that the change detection test will be relative and always will depend on the selected baseline. The baseline and the testing sequence can be expressed as follows:

Baseline sequence: x_t for $t = 1, 2, \cdots, m$

Testing sequence: x_t for $t = m+1, m+2, \cdots, n$

For $m \geq 30$ and $n - m \geq 20$

where x_t represents the anomalies of the underlying climate indicator at time *t*; m is sample size of the baseline, and n is the total number of available observations of the climate indicator.

c) Identifying the ARMA model. Most of the climate indicators and meteorological variables are a sequence of autocorrelated time series. For instance, the baseline of anomalies of air temperature, sea level pressure, sun radiation, CO_2, and O_3 are autocorrelated processes and can be represented by an ARMA model. The baseline will be tested first to determine whether or not the baseline is an autocorrelated or a white noise process. If the underlying process is a white noise the ARMA model is not required. On the other hand, if the baseline is autocorrelated then it will be used to identify an ARMA model. It should be noted that the baseline must be a stationary process. Stationary in the sense that the mean and the autocorrelation function will not change over time. This assumption is satisfied because the climate with internal natural variability will exhibit a process with constant mean and autocorrelation function independent of time. The main purpose of identifying an ARMA model is to remove the autocorrelation structure. The identification of an ARMA model can be easily accomplished by using the methodology described in several time series textbooks (Box and Jenkins 1976). An ARMA model is developed by using the historical observations to estimate the current observation. This process is known as the autoregression. If the deviation of the estimated from the observations is small the model will be called autoregressive model. On the other hand, and if a significant deviation occurs in the estimation the errors and the historical observations are used to estimate the current observation and this model is called autoregressive moving average model. Several statistical softwares are available to perform an automatic identification of the ARMA model: for instance: Statgraphics, ITMS2000. Other alternative is to use Matlab which includes the system identification toolbox that provides an excellent tool to identify the ARMA model. A typical representation of an ARMA model is as follows:

$$x_t = \frac{\theta_1 B + \theta_2 B^2 + \cdots + \theta_q B^q}{\phi_1 B - \phi_2 B^2 + \cdots + \phi_p B^p} a_t \quad (1)$$

$$\text{for} \quad t = 1,2,\cdots,m$$

Where x_t and m as defined previously; θ's and ϕ's are the parameters of the moving average and the autoregressive components of the model, respectively. The values of p and q define the order of the two polynomials; B is the back shift operator; a_t is a sequence of independent random variables with mean equal to zero and a standard deviation equal to one. It should be noted that x_t is the anomalies of the climate indicator, i.e., the periodicity component is already removed and the baseline is likely to be a stationary process.

d) Computing the ARMA fingerprint. The ARMA fingerprint is the sequence created by the difference at each point in time between the estimated from the ARMA model and the observed value. The ARMA fingerprint can be computed as follows:

$$f_t = x_t - \hat{x}_t \quad \text{for} \quad t = 1,2,\cdots,n \quad (2)$$

$$\hat{x}_t = \frac{\hat{\theta}_1 B + \hat{\theta}_2 B^2 + \cdots + \hat{\theta}_q B^q}{\hat{\phi}_1 B - \hat{\phi}_2 B^2 + \cdots + \hat{\phi}_p B^p} \hat{a}_t \quad (3)$$

where f_t is the ARMA fingerprint; $\hat{a}_t$ are the residuals for the baseline sequence; $\hat{\theta}$'s and $\hat{\phi}$'s are parameter estimates that must be computed with the baseline sequence and must be unchanged for $t = 1,2,\cdots,n$. Again appropriate software to perform this calculation is Matlab (Mathwork 2000).

Thus, if no change has occurred in the underlying process then the fingerprint will reduce to residual values $(f_t = \hat{a}_t)$, and will behave as a white noise sequence. However, if the process exhibits a significant change, the ARMA model will show a unique characteristic which will be exhibited either in the mean or in the autocovariance function of the given sequence and this special sequence will be called the ARMA fingerprint. Thus, if a significant change occurs in the mean of the process, the ARMA fingerprint will also exhibit a significant change in the mean. On the other hand, if change occurs in the second moment of the process, the fingerprint will exhibit significant change in the autocorrelation function (Ramirez, and Sastri, 1997).

e) Sequential Hypothesis Testing. If the climate indicator was forced by external forces, its

ARMA fingerprint will present a trend in the mean or a significant change in the autocorrelation structure. Thus to detect these changes two sequential tests are needed. Since the climate changes are represented by a small variation either in the mean or in the autocovariance, the tests must be very sensitive. In addition since the decision of the hypothesis testing is at each point in time, the exponentially weighted moving average (EWMA) and the transient detection test are adopted to detect the climate change. EWMA test was proposed by Roberts (1959) and the transient test was proposed by Ramirez and Sastri (1997). In this study only the EWMA test is implemented, the transient test will be applied in a future work.

The exponential weighted moving average test can be expressed as follows:

$$z_t = \lambda f_t + (1-\lambda) z_{t-1} \qquad (4)$$

A significant increment occurs in the mean at time t if $z_t > U_t$ and a significant decrement occurs in the mean at time t if $z_t < L_t$, where

$$U_t = \mu + M\sigma\sqrt{\frac{\lambda}{2-\lambda}\left[1-(1-\lambda)^{2t}\right]}, \qquad (5)$$

$$L_t = \mu - M\sigma\sqrt{\frac{\lambda}{2-\lambda}\left[1-(1-\lambda)^{2t}\right]} \qquad (6)$$

for $t = 1,2,\ldots,n$

where f_t is the ARMA fingerprint at time t, μ and σ are the mean and the standard deviation of the baseline sequence of f_t for t=1,2,…,m; z_t is the exponentially weighted moving average of the fingerprint, and the initial value of z_t can be estimated by the average of the fingerprint during the baseline (t=1,2,…,m); λ is a weighted constant and varies between zero and one. However, to have better results it is recommended to take the value of 0.2. and M is constant that change depending on λ. Thus, for $\lambda = 0.2$ $M = 3$.

The EWMA test was adopted because it is an efficient test to detect a small shift in the mean and also because it is robust test in the senses that it is not affected by moderate deviations from the Gaussian process and because it is not affected by weakly autocorrelated time series. Cumulative sum (CUSUM) test can also be used to detected climate change (Page 1954). However, since the implementation EWMA is easier than the CUSUM and detection results are about the same the EWMA test is recommended. An excellent discussion of the implementation of these tests can be found in Montgomery, (2001)

4. PRELIMINARY RESULTS

4.1 Attribution variables

a) Sunspots. The algorithm for detecting climate change was applied to identify whether or not the sunspots attribution variable exhibits a significant change on the mean. The sunspots reveal a significant trend with an increasing rate of 0.39 sunspots per year. Sunspots are dark holes in the sun creating larger increment of sun brightness in the surrounding areas, and the overall effect is the more sunspots the more solar radiation, (visit the web site for information: http://en.wikipedia.org/ wiki/Sunspot). She et al (2004) pointed out that there is a relationship between temperatures observed in mesopause and the effect of solar cycle. They also pointed out that the volcanic eruption and solar flux variability affect mesopause region temperatures.

After removing the trend and the seasonal component the ARMA fingerprint technique was implemented and the monthly stochastic component shows a significant increment during 1947 to 1960 and especially on December 1957. The annual time series also indicates a significant increment in 1957. Figure 10 shows results for the monthly and annually time series.

b) Carbon Dioxide. The carbon dioxide shows a strong trend and seasonality components. The rate of change shows on the average an increment of 0.79 ppm (see Figure 3). Figure 11 shows that after removing trend and seasonality components the annual stochastic behavior do not exhibit any additional change.

The sunspots and CO_2 exhibited a significant trend during the evaluated period. In addition the sunspots revealed an additional increment on solar activity during 1947 to 1960. Thus, the recorded global warming may be associated with the increasing trend of both the sunspots and CO_2 concentrations.

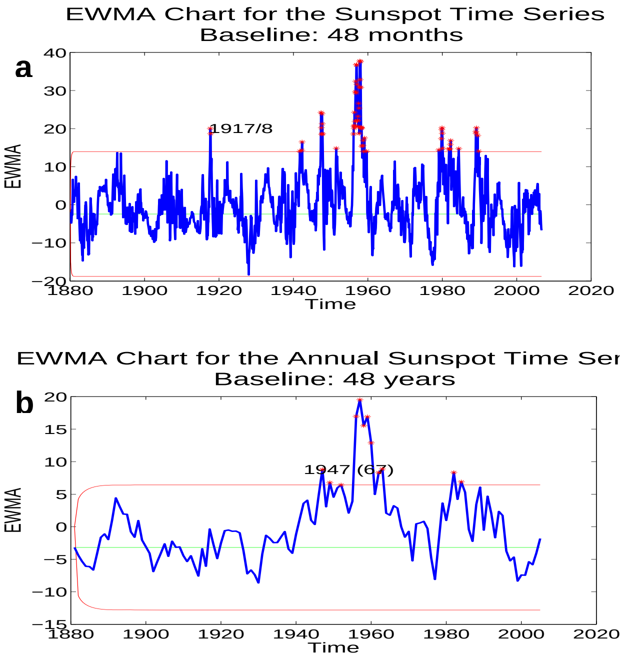

Figure 10 The analysis of sunspots. a The monthly time series shows a significant increment on solar activity on Decembere 1957. b The annual time series shows a significant change on 1957. The first increment of solar activity started 1947 and finished on 1960. The second increment started on 1982 and finished on 1984 and the second increment was smaller than the first one.

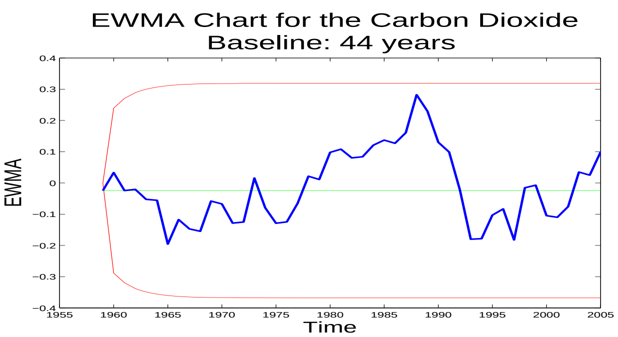

Figure 11 Annual carbon dioxide. No significant change was detected.

4.2 Climate indicator variables

a) Global Surface temperature. The surface temperatures show an increasing trend of 0.0106, 0.0099 and 0.0138 ºF per year for the global land, the global ocean and lad, and the North Hemisphere land temperature, respectively. After removing the trend the stochastic component shows that surface temperature exhibits a significant reduction about 1970 and after that a persistent increment is exhibited and becomes a significant increment about 2002.

Figure 12 shows that the statistical test reveals a clod period from 1968 to 1979 and the hottest period from 2002 to 2005.

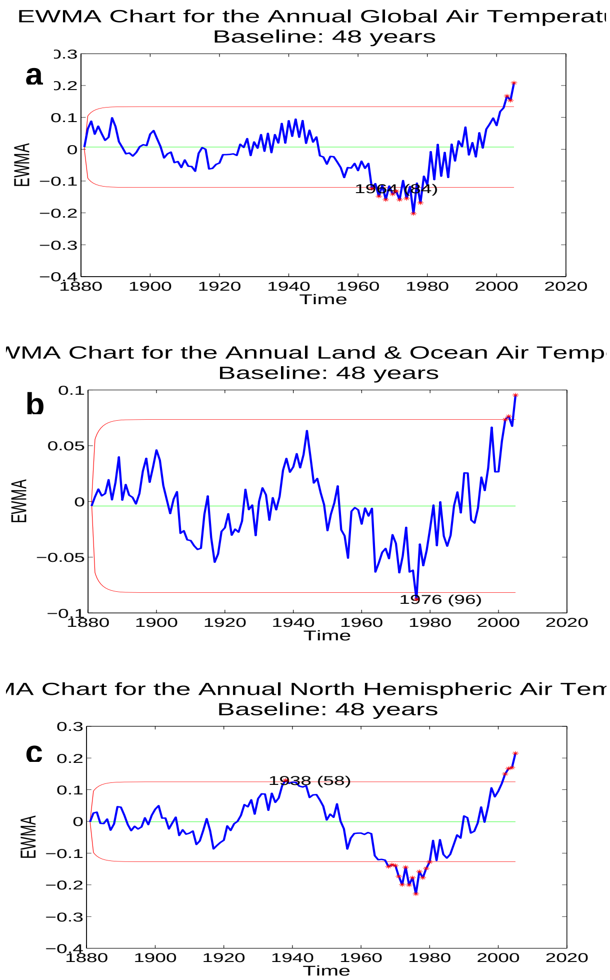

Figure 12 Annual mean surface temperature (ST). a, the global data show that the cold period started in 1964 and finished on 1979 and the hottest period started on 2002 up to present time (2006). b, the land and ocean data exhibit a punctual cold time in 1976 and the hottest period from 2002 to present time. c, the north hemisphere data shows that cold period from 1968 to 1979 and a more intense the hottest period started in 2002 until present.

b) Caribbean air temperature. Puerto Rico exhibits an increasing rate of temperature of about 0.0193, 0.0147 and 0.0254 ºF for the annual mean, maximum, and minimum temperature, respectively. Figure 13 shows that the minimum air temperature is increasing faster that maximum air temperature. The statistical test was implemented to the difference between the maximum and the minimum air temperature and it was found that in Puerto Rico a significant increment was identified in 2004. Figure 13 shows evidences of this result.

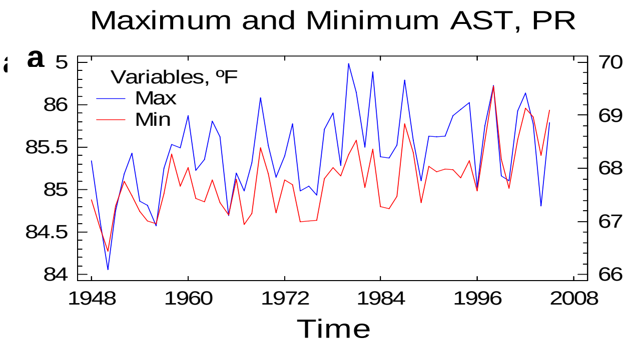

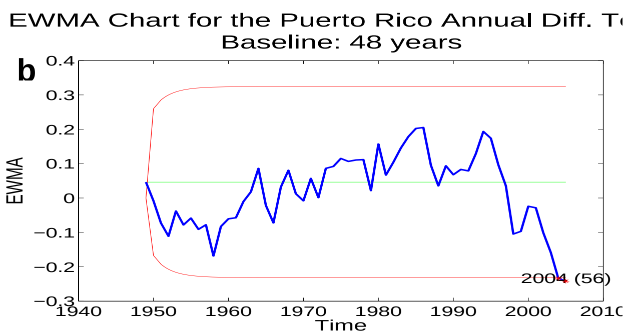

Figure 13 a shows the maximum and the minimum air temperatures for Puerto Rico. The scale on the left is for the maximum and the scale on the right is for the minimum air temperature. b, the maximum minus the minimum air temperature shows a significant change that occurred in 2004.

This is an ongoing project and results for the remaining Caribbean islands are not available yet.

b) Global and Caribbean cloud cover. It was found that the total cloud cover is decreasing at the rate of -0.17 % per year. It was also noted that low clouds have a larger decreasing rate than the other clouds. Figure 14 shows that in addition to the decreasing trend the middle cloud stochastic component shows a significant cloud reduction during the period 1993 to 1998.

The Caribbean clouds cover shows a significant reduction of about -0.38 % per year. Again the significant reduction on Caribbean cloud amount is observed in the low clouds, about -0.17% per year. The stochastic component does not show any additional change.

c) Global and Caribbean sea level. The global sea level is increasing at the rate of 3 mm per year. In addition the stochastic component shows two significant increments one in November of 1997 and the second in January 1998. Hansen (2005) argue that during this period of time the sea level rises due to instable energy balance. The Earth is now out of energy balance by close to +1 W/m2, i.e., with that much more energy absorbed from sunlight than the energy emitted to space as thermal radiation .This large growing planetary energy imbalance has no known precedent, greatly exceeding the global mean energy imbalance associated with changes of the Earth's orbital elements that paced the natural building and decay of ice sheets.

The Caribbean sea level has no trend and the stochastic component shows a significant increment on March 1998. This event is may be associated to the strong El Nino event that occurred in 1997. Figure 15 shows the sea level change at global and Caribbean scale.

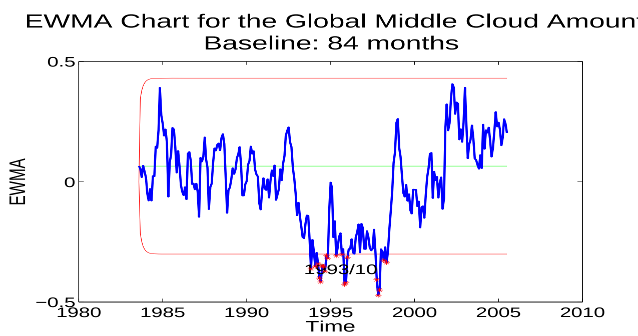

Figure 14 The detection test shows the middle clouds have a significant cloud reduction during 1993 to 1998.

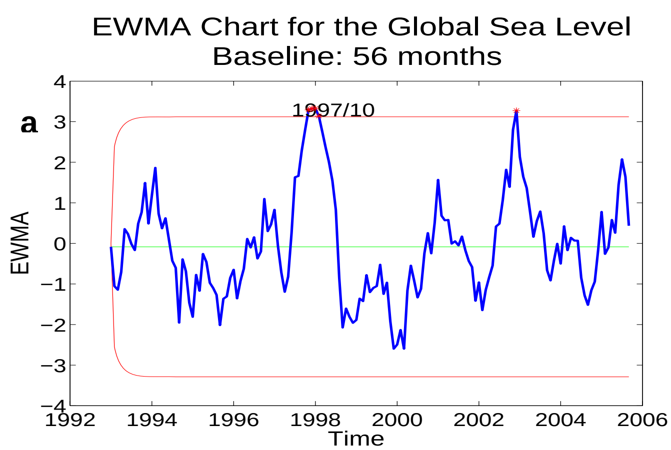

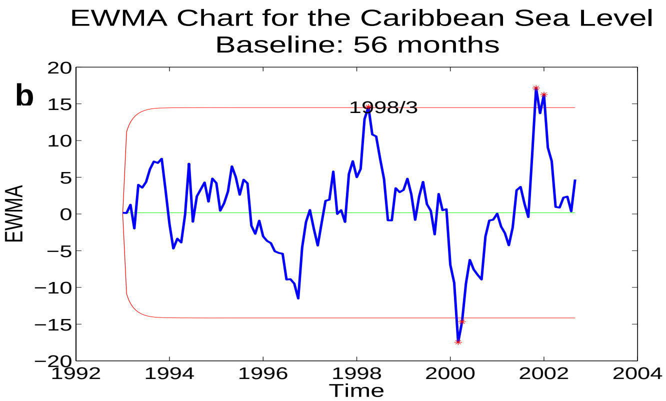

Figure 18 a. The statistical test show two significant changes on the global sea level one in 1997 and the second one in 2003. Statistical test apply to the sea level change, and **b** the sea level at the Caribbean scale shows two significant changes one that occurred in 1998 and the second one 2002.

5. CONCLUSIONS.

Climate variability which is not forced by external factors is known as internal climate variability and occurs at all times from weeks to centuries. External factors that force climate variations are due to natural and anthropogenic causes, such as solar radiation, and increasing concentration of greenhouse gases. Climate change detection is the procedure to determine when an observed climate behavior differs significantly from the internal natural variability.

The North Hemisphere shows a significant increment on air temperature that occurred in 2002 and the major Caribbean islands shows a significant increment of minimum air temperature in 2004. A sequential statistical test shows that the temperature trends over the North Hemisphere started in 1970 while in the Caribbean started in 1995. Monthly data were obtained from Goddard Institute for space Studies (1880-2004), cooperative observed network (1948-2005), global historical climatology network (1948-2005) and from NCEP/NCAR reanalysis data (1948-2005).

The global sea level time series shows a positive linear trend with an average increment of about 3 mm per year, while the Caribbean does not exhibit a trend. The sea levels at global and Caribbean regional scale have shown a significant increment at the same point in time1998. The studied data was obtained from TOPEX Microwave Radiometer and Jason satellite observations from 1992 to 2005.

The global and Caribbean cloud cover is decreasing and especially this effect is shown over the low clouds. The cloud cover monthly time series was obtained from the International Satellite Cloud Climatology Project. The time series covers the period from July 1983 to June 2005.

A sequential statistical test has been introduced to detect when as significant climate change has occurred. The test is very simple and efficient and consists of removing the autocorrelation structure of the process and determines when the fingerprint of the process exhibits a significant change. The major contribution of this work is to introduce a tool to determine without ambiguity when a climate change has occurred.

6. ACKNOWLEDDGEMENTS

This research has been supported by NASA-EPSCoR grant NCC5-595 and also by the University of Puerto Rico. Authors want to recognize the technical support from several institution that the provided the climate indicator variables.

REFERENCES.

Angeles-Malaspina, Moisés E. 2005. An Assessment of Future Caribbean Climate Change Using "Business as Usual" Scenario by Coupling GCM Data and RAMs. Thesis of Master of Science in Mechanical Engineering, University of Puerto Rico-Mayagüez Campus.

Barnett, T.P. Hasselman, K., M. Chelliah, T. Delworth, G. Hergel, P. Jones, E. Ramsmusson, E. Roeckner, C Ropelewski, B. Santer and S. Tett (1999), Detection and Attribution of Recent Climate Change: A Status Report, *Bull. Am. Meteorol. Soc.* Vol. 80 No. 12, December 1999.

Battisti D., Bitz M., Moritz R. (1997) Do General Circulation Models Underestimate the Natural Variability in the Arctic Climate? Journal Climate, Vol. 10: 1909 – 1920.

Box G., and Jenkins (1976). Time Series Analysis Forecasting and Control. Golden-Day, California.

Brockwell, P. and Davis R. (2002), Introduction to Time Series and Forecasting, 2nd ed., Springer-Verlag New York, Inc.

Changnon S. A., Pielke R. A. Jr., Changnon D., Sylves R. T., and Pulwarty R., (2000) Human Factors Explain the Increased Losses from Weather and Climate

Extremes; *Bull. Am. Meteorol. Soc.*; 81, 437 – 442.
Easterling D. R., Meehl G. A., Parmesan C., Changnon S. A., Karl T. R. and Mearns L. O. (2000) Climate Extremes: Observations, Modeling, and Impacts; *Science*, 289, 2068 – 2074.
Hansen, J (2005). A slippery slope: How much global warming constitutes “dangerous anthropogenic interference”? *Climatic Change*, 68: 269–279.
Huntingford C., Stott P., Allen M., and Lambert H., (2006) Incorporating model uncertainty into attribution of observed temperature change, Geophys. Res. Lett., Vol. 33, L05710.
IPCC, Climate Change 2001: The Scientific Basic, Cambridge University Press, 697 – 738 pps.
Keeling, D. and Whorf T. (2005). Atmospheric CO2 records from sites in the SIO air sampling network. In Trends: A Compendium of Data on Global Change. Carbon Dioxide Information Analysis Center, Oak Ridge National Laboratory, U.S. Department of Energy, Oak Ridge, Tenn., U.S.A. Available in wet site: http://cdiac.ornl.gov/trends/co2/sio-mlo.htm
Leuliette, E. , R. Nerem, and G. Mitchum, (2004). Calibration of TOPEX/Poseidon and Jason altimeter data to construct a continuous record of mean sea level change. *Marine Geodesy*, 27(1-2), 79-94.
MathWorks, 2000: *Optimization Toolbox for use with Matlab: User’s Guide.* The MathWorks, Inc**.**
Montgomery, D. (2001), Introduction to Statistical Quality Control, 4th Edition, John Wiley & Sons, Inc.
Quispe, W. (2006). Sieve Bootstrap en Series de Tiempo de Nubosidad en el Caribe. Tesis de Maestria en Ciencias en Matematica, Universidad de Puerto Rico-Recinto de Mayagüez.
Ramirez N. and Julca O. (2006), Detection of a Local Climate Change, *86th AMS Conference*, P2.14.
Robock A. (2000). Volcanic Eruptions and Climate, Reviews of Geophysics, 38, 2: 191–219.
Salinger, M. J. (2005), “Climate Variability and Change: Past, Present and Future – an overview”, Climate Change 70: 9-29.
Schar C, Vidale Pl, Luthi D, Frei C, Haberli C, Liniger MA, and C. Appenzeller, (2004); The role of increasing temperature variability in European summer heatwaves; *Nature*, 427: 332-335.
Stott P. and Kettleborough J., (2002). Origins and estimates of uncertainty in predictions of twenty-first century temperature rise, Nature, Vol. 416: 723 – 726.
She C., Krueger D., (2004), Impact of natural variability in the 11-year mesopause region temperature observation over Fort Collins, CO (41_N, 105_W), Advances in Space Research, Vol. 34, 330–336.